



A dual-band slotted trapezoidal inverted-F antenna for indoor WLAN communications

Downloaded from: <https://research.chalmers.se>, 2025-12-06 04:12 UTC

Citation for the original published paper (version of record):

Pang, F., Yin, J., Chen, W. et al (2016). A dual-band slotted trapezoidal inverted-F antenna for indoor WLAN communications. Progress In Electromagnetics Research Letters, 64: 57-63.
<http://dx.doi.org/10.2528/PIERL16101305>

N.B. When citing this work, cite the original published paper.

A Dual-band Slotted Trapezoidal Inverted-F Antenna for Indoor WLAN Communications

Feng Pang^{1,2}, Jungang Yin^{3*}, Wei Chen³, Jian Yang⁴, Chao Xie³ and Xiang Li³

¹National Astronomical Observatories of Chinese Academy of Sciences, Beijing, 100012, China

²University of Chinese Academy of Sciences², Beijing, 100049, China

³Dept. of Electronics at Hunan University, Changsha, 410082, China

⁴Dept. of Signals and Systems at Chalmers University of Technology, Gothenburg, S-412 96, Sweden

Abstract—This letter presents a new directional dual-band slotted trapezoidal inverted-F antenna (IFA) for indoor Wireless Local Area Network (WLAN) applications. The dual-band performance can be obtained by tuning the lengths of the inner symmetrical trapezoidal slots and the outer trapezoidal arms in a nearly independent manner. The measured results show that the proposed antenna can provide two separate impedance bandwidths (return loss better than 10 dB) of around 180 MHz and 750 MHz for 2.4/5.1-5.8GHz WLAN bands, respectively. Good radiation performance and roughly constant in-band antenna directivities are also observed.

Key Words—Dual WLAN bands, Slotted Trapezoidal IFA

I. INTRODUCTION

Multiband or wideband antennas have increasingly attracted great attention in the wireless industry as so many different wireless technologies develop rapidly. A large number of antennas have been designed for wireless local area network (WLAN) applications [1]-[5]. Most of them have omnidirectional radiation patterns as applied to wireless terminals, such as mobiles, pads, laptops and so on. For indoor wireless access points or point-to-point communications, however, it is often required that the antenna is somewhat directional to allow the installation of the antenna against a wall or on a ceiling surface [6]-[8]. Slotted structures are often used to realize the multi-band performance [9]-[11], in particular for dual-band patches [12]-[13]. One resonance is due to the fundamental mode of the main patch, while the currents along slot edges introduce an additional resonance.

In this letter, we present a new directional dual-band slotted trapezoidal planar inverted-F antenna, with low profile and low manufacture cost, and capable of covering the 2.4/5.1-5.8GHz dual WLAN bands for indoor communications.

II. ANALYSIS AND SIMULATION

The geometry of the proposed dual-band slotted trapezoidal inverted-F antenna is presented in Fig. 1. The proposed antenna has been simulated and optimized by using *CST MWS*. The simulated surface current distribution shown in Fig. 2 implies that a dual-band performance can be obtained by tuning the two inner symmetrical trapezoidal slots and the outer trapezoidal arms

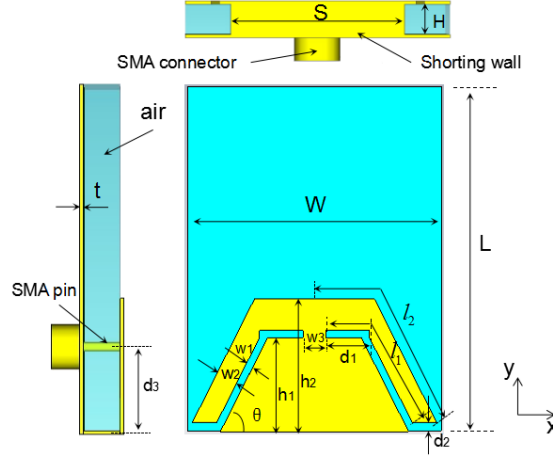


Fig. 1 Geometry of the proposed antenna (yz-plane is the E-plane while xz-plane is the H-plane)

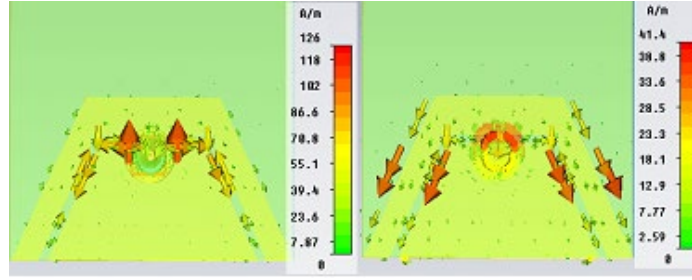


Fig. 2 Simulated surface current distribution: (a) at 2.4 GHz; (b) at 5.5 GHz.

The lower and upper resonance frequencies are primarily related to the length l_1 of the inner slots and the length l_2 of the outer arms, and can be approximated by the following empirical expressions based on the simulations, in a similar format as in [14]:

$$f_L \approx \frac{c}{2 \times (3 \times l_1)} \quad (1)$$

$$f_H \approx \frac{c}{2 \times l_2} \quad (2)$$

where

$$l_1 \approx \frac{h_1}{\sin \theta} - \frac{d_2}{\sin \theta} + d_1 - w_1 \quad (3)$$

$$l_2 \approx \frac{h_2}{\sin \theta} - \frac{d_2}{\sin \theta} + \frac{w_3}{2} + d_1 + w_1 \quad (4)$$

c is the light speed in free space, f_L and f_H are the lower and upper resonance frequency, respectively.

Exhibited in Fig. 3 are the comparisons of the resonance frequencies f_L and f_H , respectively, between calculations by the abovementioned empirical expressions and *CST* simulations. As good agreement is observed, the expressions (1)-(4) could be considered as a guideline in the initial design of the antenna geometry.

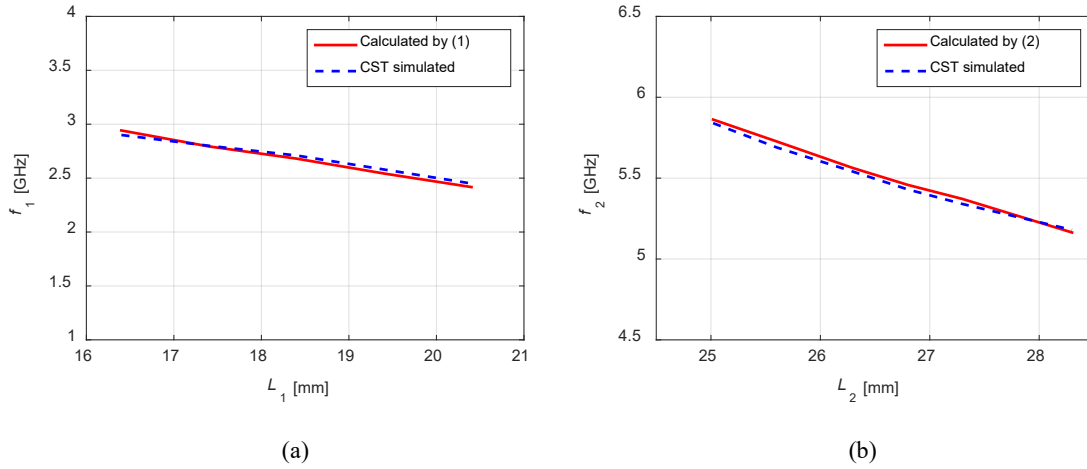


Fig. 3 Comparisons of resonance frequency between calculations by expressions (1)-(2) and *CST* simulations: (a) f_L ; (b) f_H .

A parameter sweeping for S_{11} performance over all parameters included in (1)-(4) has been carried out. It is found from Figs. 4-8 that the resonance tips over both the lower and upper bands tend to be sensitive to the parameters h_1 and d_2 . However, h_2 and θ affect the S_{11} tip primarily in the upper band while hardly in the lower band. In contrast, d_1 affect the S_{11} tip primarily over the lower band but little over the upper band. In other words, the variation of h_1 and d_2 affects the S_{11} performance over both the lower and upper bands; the change of d_2 and θ affect the performance only in the lower band while d_2 affects the performance only in the upper band. Consequently, the antenna geometry can be designed in such a scheme that h_1 and d_2 are first tuned to roughly fix the dual band, while h_2 , θ and d_1 are then fine-tuned to improve the S_{11} performance in dual bands in a nearly independent manner.

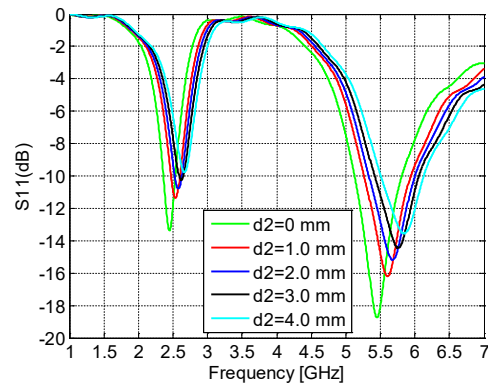


Fig. 4 Sweeping of d_2 for S_{11} while other parameters set as in Table I

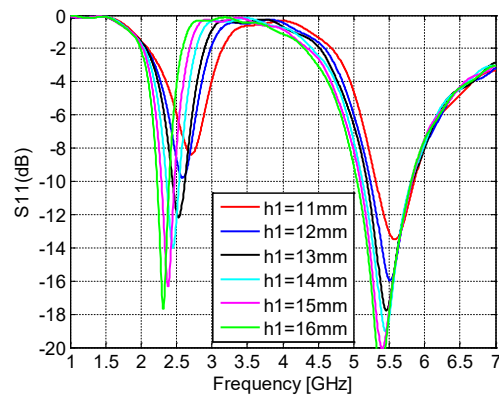


Fig. 5 Sweeping of h_1 for S_{11} while other parameters set as in Table I

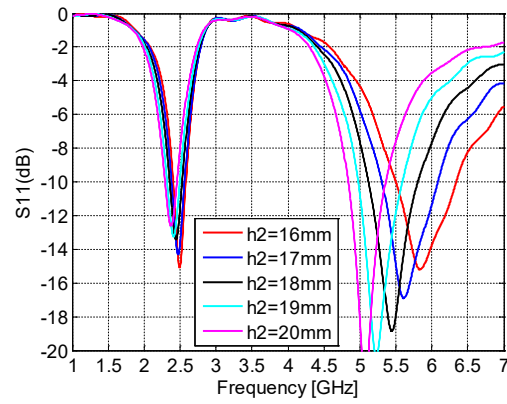


Fig. 6 Sweeping of h_2 for S_{11} while other parameters set as in Table I

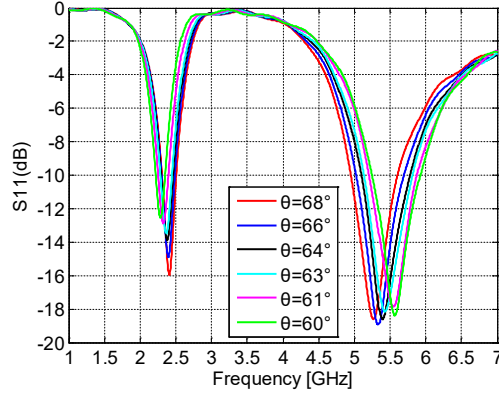


Fig. 7 Sweeping of θ for S_{11} while other parameters set as in Table I

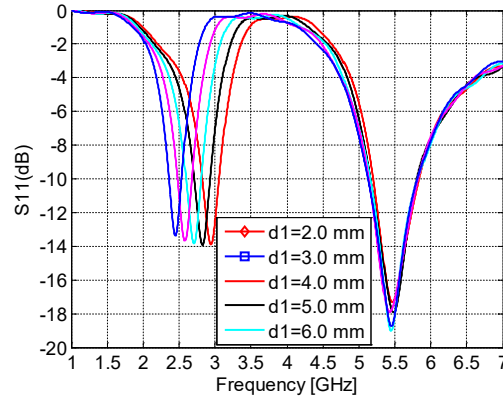


Fig. 8 Sweeping of d_1 for S_{11} while other parameters set as in Table I

The optimized geometrical parameters are listed in Table I. As can be seen, its total size is $47.0 \times 35.0 \times 4.5 \text{ mm}^3$, which is much thinner than that ($43 \times 26 \times 12 \text{ mm}^3$) of a 2.4/5.8GHz dual-band directional antenna proposed in [8] for RFID reader applications, and much more compact than that ($57 \times 57 \times 21 \text{ mm}^3$) of a 2.5-4.8GHz slot antenna designed for WLAN systems in [10].

TABLE I GEOMETRIC PARAMETERS OF THE PROPOSED ANTENNA

Parameter	Value	Parameter	Value
S	23.0 mm	$w1$	1.0 mm
H	4.5 mm	$w2$	3.0 mm
W	35.0 mm	$w3$	3.2 mm
L	47.0 mm	$d1$	6.0 mm
θ	63.0°	$d2$	0.0 mm
$h1$	13.8 mm	$d3$	11.5 mm
$h2$	18.5 mm	t	0.1 mm

III. MEASURED RESULTS

As can be seen in Fig. 9, the fabricated trapezoidal inverted-F antenna is made of copper and probe-fed through an air cavity by an SMA connector, which is low-profile, low-cost and easy to fabricate.

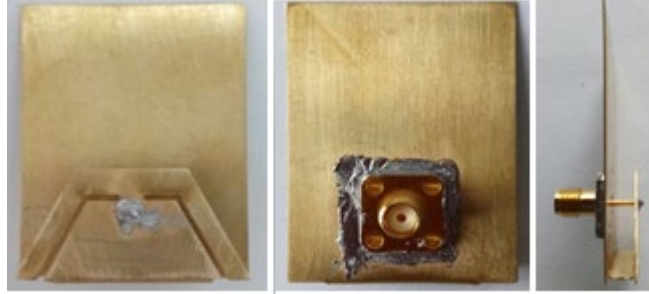


Fig. 9 Top/bottom/side view of the fabricated antenna prototype.

The measured and simulated reflection coefficients of the proposed antenna are demonstrated in Fig. 10. The measured bandwidth defined by return loss better than 10 dB (10dB impedance bandwidth) is around 180 MHz (2.41-2.59 GHz) and 750 MHz (5.01-5.76 GHz) at dual bands, respectively. It is observed that the measured results agree very well with the simulated results. The slight deviation is due to the tolerances, deformation and soldering, which cause some perturbation to the cavity. The measured 10dB bandwidths are sufficiently large to fully cover the dual WLAN bands.

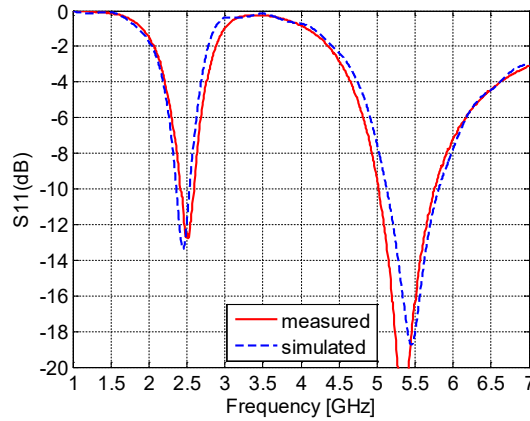


Fig. 10 Simulated and measured S_{11} parameters of the proposed antenna

The far-field patterns were measured in an anechoic chamber with the Agilent antenna-measurement system. The measured E- and H-plane co-polar patterns at 2.44/5.2/5.5/5.8 GHz are displayed in Fig. 11.

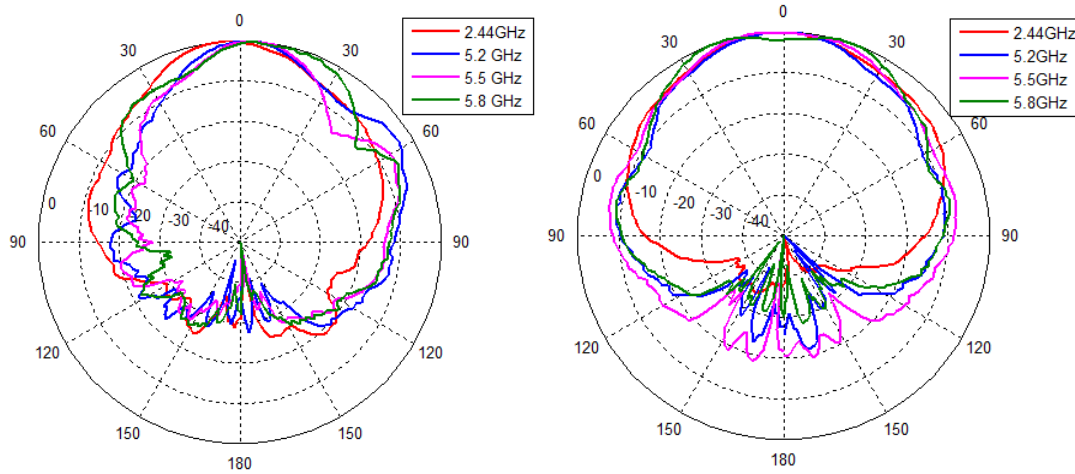


Fig. 11 Measured co-polar patterns in E-plane (left) and in H-plane (right) at different frequencies

Listed in Table II are the measured co-polar directivities at certain frequency points in the lower and upper bands. The simulated and measured co-polar directivities in the upper band are shown in Fig. 12. It can be seen that the directivities vary from about 6.1 to 8.3 dBi between 5.1-5.8 GHz, and good agreement is observed between the measured results and the simulated results. The deviation is due to accessories for measurement setup, such as the supporting plate, poles, screws, cables, etc.

TABLE II MEASURED DIRECTIVITIES IN DUAL BANDS

Frequency (GHz)	Directivity (dBi)	Frequency (GHz)	Directivity (dBi)
2.40	6.1	5.10	7.2
2.44	5.7	5.50	7.5
2.50	6.0	5.80	6.1

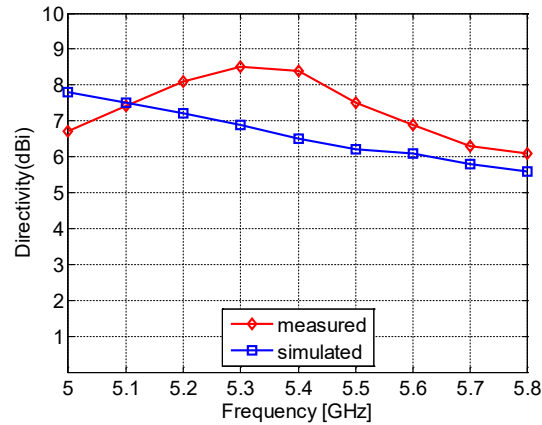


Fig. 12 Measured and simulated antenna directivities in upper band.

The radiation efficiency of the antenna prototype, which is a measure of its ohmic losses, as well as the total radiation efficiency that takes both its ohmic and mismatch losses into account, was measured in a Bluetest reverberation chamber [15], where the measurement uncertainty is 0.5 dB [16]. The measured data were obtained by using a rigorous calibration method presented in [17]. It can be

observed from Fig. 13 that the measured radiation efficiency is about -0.5 dB over both the lower and upper bands; the measured total radiation efficiency is higher than -0.7 dB over the upper band, while it is higher than -1.0 dB over the lower band, which is due to a bit worse matching performance in the lower band than that in the upper band.

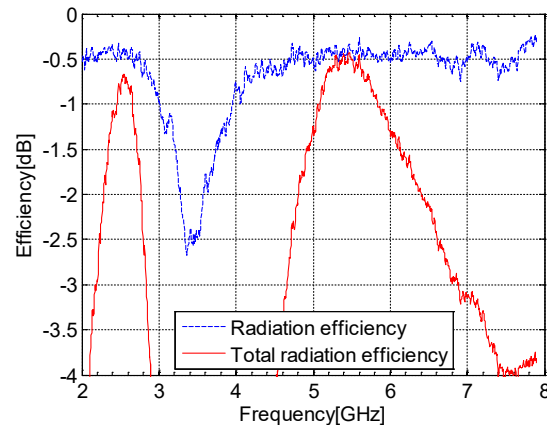


Fig. 13 Measured radiation efficiencies over the dual bands.

IV. CONCLUSION

A new directional dual-band slotted trapezoidal inverted-F antenna has been proposed and studied in this letter. The simple formulas as design guidelines for the dual resonance frequencies are provided. The measurement results of the prototype agree well with the simulation results. About 180/750 MHz bandwidths defined by return loss better than 10 dB are obtained at 2.4-2.5/5.1-5.8GHz WLAN bands, respectively. Around 6.0 dBi directivities are observed at the lower band while 6.1-8.3 dBi at the upper band. The measured total radiation efficiencies are better than -0.7 dB over the upper band, while better than -1.0 dB over the lower band. Besides, the proposed antenna is low-profile, low-cost and easy to fabricate, making it ready to be applied in indoor WLAN communications.

V. ACKNOWLEDGMENTS

This work was supported by Chinese Ministry of Science and Technology under grant No.2013CB837900, by National Science Foundation of China under grant No.11261140641 and 11503049, by Chinese Academy of Sciences under grant No.KJZD-EW-T01, and by Hunan University under the Youth Researcher Growth Program.

REFERENCES

- [1] Y.-L. Kuo and K.-L. Wong, "Printed double-T monopole antenna for 2.4/5.2 GHz dual-band WLAN operations," *IEEE Trans. Antennas Propag.*, vol. 51, no. 9, pp. 2187–2192, Sep. 2003.
- [2] J.-Y. Jan and L.-C. Tseng, "Small planar monopole antenna with a shorted parasitic inverted-L wire for wireless communications in the 2.4, 5.2 and 5.8-GHz bands," *IEEE Trans. Antennas Propag.*, vol. 52, no. 7, pp. 1903–1905, Jul. 2004.

- [3] K.-L. Wong, L.-C. Chou and C.-M. Su, "Dual-band flat-plate antenna with a shorted parasitic element for laptop applications," *IEEE Trans. Antennas Propag.*, vol. 53, no. 1, pp. 539–544, Jan. 2005..
- [4] H. Zhang and H. Xin, "A dual-band dipole antenna with integrated balun," *IEEE Trans. Antennas Propag.*, vol. 57, no. 3, pp. 786–789, Mar. 2009.
- [5] Y.-K. Shih, W.-J. Liao, S.-H. Chang, P.-C. Chiang, C.-T. Yeh, and T.-G. Ma, "A Four Element Antenna System with Antenna Diversity for Dual Band WLAN Operation," *Proceedings of 2013 URSI International Symposium on Electromagnetic Theory (EMTS)*, pp. 679-682, May. 2013.
- [6] R. Gardelli, G. La Cono, and M. Albani, "A low-cost suspended patch antenna for WLAN access points and point-to-point links," *IEEE Antennas Wireless Propag. Lett.*, vol. 3, pp. 90–93, 2004.
- [7] C. R. Medeiros, E. B. Lima, J. R. Costa, and C. A. Fernandes, "Wideband slot antenna for WLAN access points," *IEEE Antennas Wireless Propag. Lett.*, vol. 9, pp. 79–82, 2010.
- [8] X. Quan, R. Li, Y. Cui and M. M Tentzeris, "Analysis and design of a compact dual-band directional antenna," *IEEE Antennas Wireless Propag. Lett.*, vol. 11, pp. 547–550, 2012.
- [9] C.-Y. Huang and E.-Z. Yu, "A slot-monopole antenna for dual-band WLAN applications," *IEEE Antennas Wireless Propag. Lett.*, vol.. 10, pp. 500–502, 2011
- [10] N. Zhang, P. Li, B. Liu, X. W. Shi, and Y. J. Wang, "Dual-band and low cross-polarisation printed dipole antenna with L-slot and tapered structure for WLAN applications", *Electron. Lett.*, no. 47, pp. 360–361, 2011.
- [11] Jeen-Sheen Row, "Dual-frequency Triangular Planar Inverted-F antenna," *IEEE Trans. Antennas Propag.*, vol. 53, no. 2, pp. 874–876, 2005.
- [12] T. Huynhand K. F. Lee, "Single-layer single-patch wideband microstrip antenna," *Electron. Lett.*, vol. 31, pp. 1310 – 1312, Aug. 1995.
- [13] Jeen-Sheen Row, "Dual-Frequency triangular planar inverted-F antenna," *IEEE Trans Antennas Propag.*, no. 53, pp. 874–876, 2005.
- [14] Z. D. Liu, P. S. Hall, and D. Wake, "Dual-frequency planar inverted-F antenna," *IEEE Trans Antennas Propag.*, vol. 45, pp. 1451–1458, 1997.
- [15] Bluetest AB [Online]. Available: <http://www.bluetest.se>
- [16] P.-S. Kildal, X. Chen, C. Orlenius and et al., "Characterization of reverberation chambers for OTA measurements of wireless devices: Physical formulations of channel matrix and new uncertainty formula," *IEEE Trans. Antennas Propag.*, vol. 60, no. 8, pp. 3875–3891, 2012.
- [17] H. Raza, J. Yang, and A. Hussain, "Measurement of radiation efficiency of multiport antennas with feeding network corrections," *IEEE Antennas Wireless Propag. Lett.*, vol. 11, pp. 89–92, 2012.